Vapor-Phase Oxidation of Ethyl Lactate to Pyruvate over Various Oxide Catalysts

Shigeru SUGIYAMA,* Naoya SHIGEMOTO, Naoki MASAOKA, Souichi SUETOH, Hideaki KAWAMI, Keiko MIYAURA,† and Hiromu HAYASHI

Department of Chemical Science and Technology, The University of Tokushima, Minamijosanjima, Tokushima 770
†Shikoku Research Institute Inc., Yashima-nishi, Takamatsu 761-01

(Received November 24, 1992)

Oxidation of ethyl lactate to pyruvate was carried out in vapor-phase over various oxides. MoO_3 showed a higher selectivity than that of the other single oxide examined. Binary oxides containing molybdenum such as Fe_2O_3–MoO_3 and TeO_2–MoO_3 showed high selectivities to pyruvate over 90% at 300 °C with high lactate conversion over 75%. The maximum activity on SnO_2–MoO_3 was observed at a low temperature of 250 °C.

Pyruvic acid (**1a**) is the simplest homologue of the α-keto acids, which were extensively reviewed by Cooper et al.[1] Some of the routes are elegantly designed for laboratory procedures in organic syntheses, but the application of catalytic processes appears to be of more recent vintage. The preparation of **1a** by dehydrative decarboxylation of tartaric acid (**2a**) with potassium hydrogensulfate first described by Erlenmeyer[2] dates back to as early as 1881 and is still useful, but the reagent $KHSO_4$ should be used as an excess powder per batch.[3] $KHSO_4$ melts at a low temperature of 197 °C,[4] and was adapted in previous papers[5,6] for vapor-phase fixed-bed operations as a silica-supported potassium disulfate catalyst ($K_2S_2O_7/SiO_2$) to obtain ethyl pyruvate (**1b**) from the tartrate (**2b**) in a good yield of 60% at 300 °C (Scheme 1).

An alternative approach to **1a** has been made by the catalytic oxidation of lactic acid (**3a**) in the aqueous phase.[7] No absorption of oxygen was observed in the oxidation of **3a** on Pd/C, while a spectacular change in oxidation activity in favor of **1a** was observed in the presence of Pb/Pd/C and related catalysts. Bypassing the expensive noble metal catalysts, another attempt at liquid-phase oxidation of ethyl lactate (**3b**) over suspended oxide catalysts was carried out at 130 °C.[8] Single oxides less common as oxidation catalysts such as TiO_2, ZrO_2, and SnO_2, and binary oxide SnO_2–MoO_3 showed high selectivities to afford **1b**.

In the present work, the oxide catalysts were applied in the vapor-phase oxidation of **3b** in a fixed-bed flow system. The selecitvity to **1b** was quite different in comparison with that observed in liquid-phase oxidation. XRD analyses for binary oxide catalysts and XPS analysis for SnO_2–MoO_3 are also described.

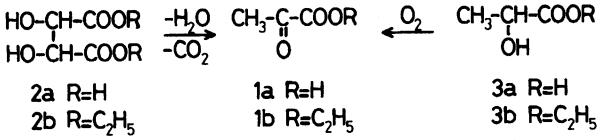

Scheme 1.

Experimental

The reaction was carried out using a conventional fixed-bed flow apparatus at 150—450 °C with a space velocity (SV) of 3600 h^{-1}. The catalyst (10—14 mesh, 2 ml) was packed in 8 mm-i.d. glass tubing inserted in an electrically-heated furnace. Substrate **3b** (5 mol%) was supplied as a toluene (45 mol%) solution by a Microfeeder (Type JP-S, Furue Science Co., Tokyo) into the reactor and diluted with a mixture of O_2 and N_2 (10 and 40 mol%, respectively). Monitoring of the reaction was done by GC (Hitachi 163-FID, Tokyo, for organic species and Yanako G-2800-TCD, Tokyo, for CO_2 and ethylene). Column packings used for GC analyses were: 15% PEG 4000/Uniport B for **1b**, **3b**, ethanol, and acetaldehyde (115 °C) and Unibeads C for CO_2 and ethylene (150 °C).

TiO_2 and ZrO_2 were obtained from Wako Pure Chemicals, Osaka, and MoO_3 from E. Merck, Darmstadt. SnO_2 was obtained by heating $Sn(OH)_2$, which was precipitated from an aqueous solution of $SnCl_2$ (Wako) by adding aqueous ammonia,[9] at 200 °C for 2 h and calcined at 500 °C for 5 h. The tin(II) hydroxide thus obtained was mixed with a solution of ammonium molybdate (Wako) to give an atomic ratio of Sn/Mo=9.[9] The paste was dried and decomposed at 300 °C for 2 h in air, and then calcined at 500 °C for 5 h to obtain SnO_2–MoO_3. An aqueous solution of ammonium molybdate and ammonium iron(III) oxalate $(NH_4)_3Fe(C_2O_4)_3 \cdot 3H_2O$ (Wako) was evaporated to dryness over a steam-bath, and the resulting mass was decomposed and calcined at 400 °C in air for 5 h to give Fe_2O_3–MoO_3 (Fe/Mo=0.25).[10] TeO_2–MoO_3 (Te/Mo=0.5) was prepared from TeO_2 (Wako) and MoO_3 by kneading with an appropriate amount of water, drying, and calcining at 500 °C in air for 5 h. Bi_2O_3–MoO_3 was prepared by the reaction of $Bi(NO_3)_3 \cdot 5H_2O$ (Wako) with ammonium molybdate.[11] The resultant paste was washed to pH=7, dried at 100 °C, and

Table 1. Surface Area, Bulk Density, and Acidity of Each Catalyst

Catalyst	Surface area $m^2\ g^{-1}$	Bulk density $g\ ml^{-1}$	Acidity mmol g^{-1}
TiO_2	12	0.72	—
ZrO_2	21	1.03	—
SnO_2	22	1.20	0.006_7
MoO_3	0.5	2.07	0.002_6
SnO_2–MoO_3	47	1.18	0.087_7
Fe_2O_3–MoO_3	4	0.62	—
Bi_2O_3–MoO_3	0.7	1.51	—
TeO_2–MoO_3	2	1.53	0.004_5

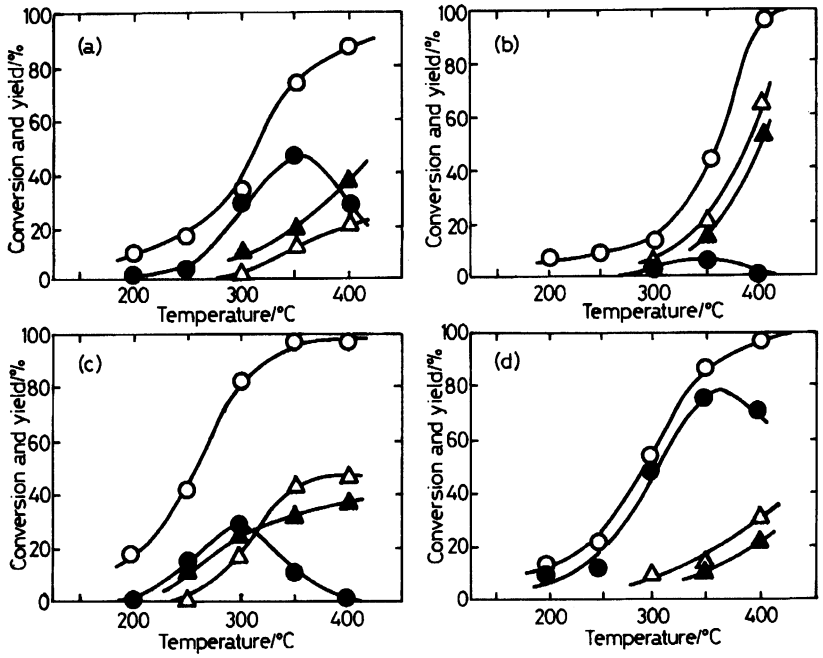

Fig. 1. Vapor-phase oxidation of ethyl lactate over single oxide catalysts. (a) TiO_2; (b) ZrO_2; (c) SnO_2; (d) MoO_3. ○, Ethyl lactate; ●, ethyl pyruvate; △, acetaldehyde; ▲, ethanol + ethylene.

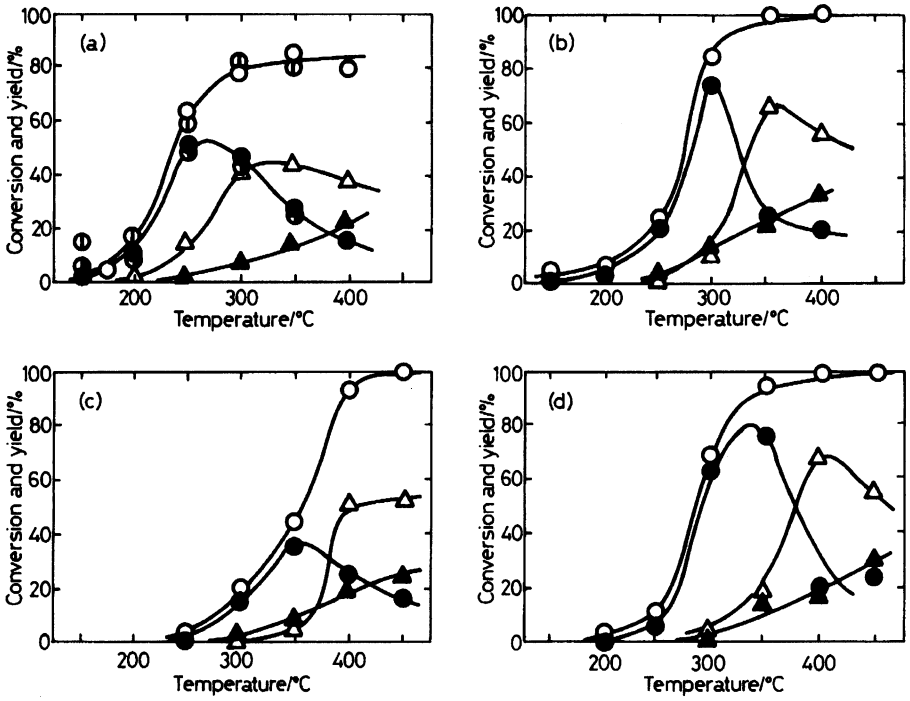

Fig. 2. Vapor-phase oxidation of ethyl lactate over binary oxide catalysts. (a) SnO_2–MoO_3; (b) Fe_2O_3–MoO_3; (c) Bi_2O_3–MoO_3; (d) TeO_2–MoO_3. Symbols as in Fig. 1 except ⊕, ethyl lactate and ◑, ethyl pyruvate in the second run.

calcined at 500 °C in air for 5 h. The surface area was determined by nitrogen adsorption (Shibata P-700, Tokyo) at liquid N_2 temperature. Acidity was measured by butylamine titration[12,13] in benzene using Dimethyl Yellow (pK_a=3.3) as an indicator. The surface area, bulk density, and acidity of each catalyst are summarized in Table 1.

Powder X-ray diffraction (XRD) was measured by the MXP system of MAC Science Co., Tokyo. X-Ray photoelectron spectra (XPS) for the Mo $3d_{5/2}$ and Sn $3d_{5/2}$ core electron of SnO_2–MoO_3 were measured by Perkin Elmer-Phi 5500 (Ulvac-phai, Inc., Chigasaki), irradiated with Mg $K\alpha$, and the observed binding energies were calibrated with 285.0 eV for a C 1s electron.

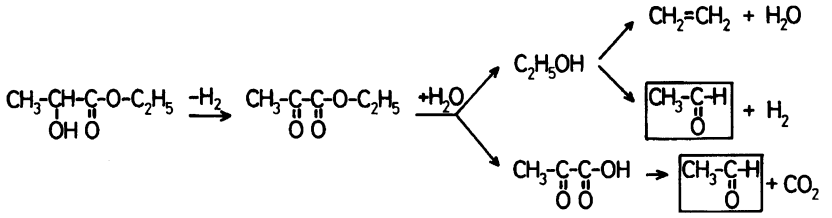

Scheme 2.

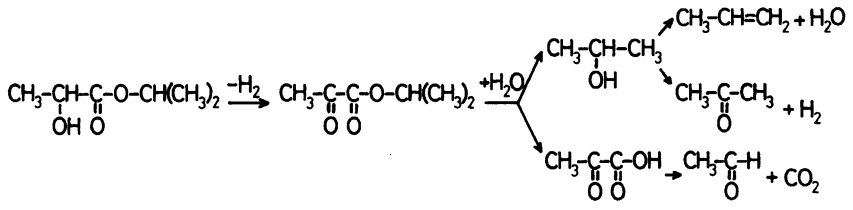

Scheme 3.

Results and Discussion

Single Oxides. In gas-phase oxidation, a wider range of reaction temperatures can be adopted than that in the liquid-phase reaction. However, since **1b** decomposes at temperatures above 350 °C,[5] selective formation of **1b** from **3b** over oxide catalysts is expected at a temperature below 300 °C.

Each single oxide showed a quite different activity for the oxidation of **3b** as shown in Fig. 1 in contrast to that in liquid-phase oxidation.[8] MoO_3 showed a high selectivity and conversion for the oxidation up to 350 °C. The reproducibility on the used catalyst re-calcined at 500 °C for 2 h after the first run was not very good. Although the oxidation occurred at less than 250 °C on TiO_2 and SnO_2 at a conversion above 19 and 44%, respectively, the selectivities at 350 °C were quite low. TiO_2 and SnO_2 possess higher activities for hydrolysis of **1b** than that of MoO_3. Since the activity for the oxidation on ZrO_2 was examined above 350 °C, overlapping to the decomposition temperature of **1b**, decomposition products of **1b** were mainly obtained on ZrO_2.

Binary Oxides. It is of interest to examine the oxidation behavior on a binary oxide, since a binary oxide catalyst often shows properties of surface area, acidity, and redox behavior quite different from the composing single oxides, providing wide possibilities for catalyst preparation.[14] Activation of lattice oxygen may be observed at high temperatures and multi-component oxide catalysts have usually been proposed for vapor-phase oxidation. Figure 2 shows the temperature effects for the oxidation of **3b** to **1b** on SnO_2–MoO_3, Fe_2O_3–MoO_3, Bi_2O_3–MoO_3, and TeO_2–MoO_3. The oxidation occurred selectively to afford **1b** on each binary catalyst. The maximum yield of **1b** on SnO_2–MoO_3 was obtained at the lowest reaction temperature among all the binary catalysts examined. The reproducibility of the used catalyst treated as for MoO_3 was excellent as shown in Fig. 2. It should be mentioned that the oxidation occurred both in the vapor phase and the liquid phase[8] only on SnO_2–MoO_3 among the examined catalysts. Fe_2O_3–MoO_3 showed the highest selectivity to **1b** around 300 °C. The activity on Bi_2O_3–MoO_3 was not very good, since the catalyst is generally active at higher temperatures. A high selectivity to **1b** was obtained up to 330 °C on TeO_2–MoO_3, but the reduction of the catalyst occurred at a high temperature even though O_2 was present in the systems and metallic Te was stuck on the reactor walls. On each catalyst, acetaldehyde, ethylene, and ethanol were obtained together with **1a** and recovered **3b**. These by-products may be afforded as shown in Scheme 2, but the origin of acetaldehyde is not clear if ethyl-substituted substrate **3b** is employed. In case of the oxidation of the isopropyl-substituted substrate, the origin of acetaldehyde may be identified easily as shown in Scheme 3. It is of interest, however, that the oxidation behavior of isopropyl lactate was quite different from that of **3b** on Fe_2O_3–

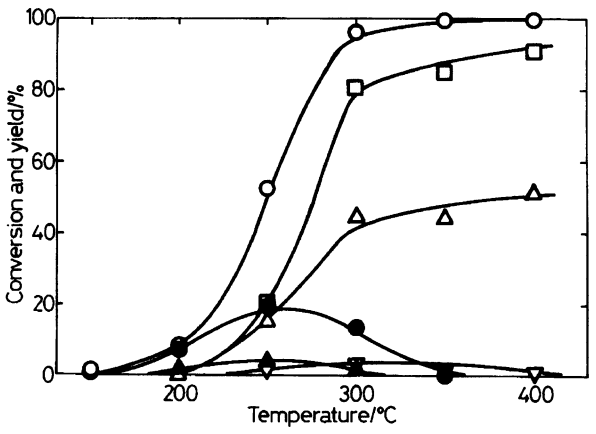

Fig. 3. Vapor-phase oxidation of isopropyl lactate over Fe_2O_3–MoO_3. ○, Isopropyl lactate; ●, isopropyl pyruvate; ▲, 2-propanol; △, acetaldehyde; ▽, acetone; □, propylene.

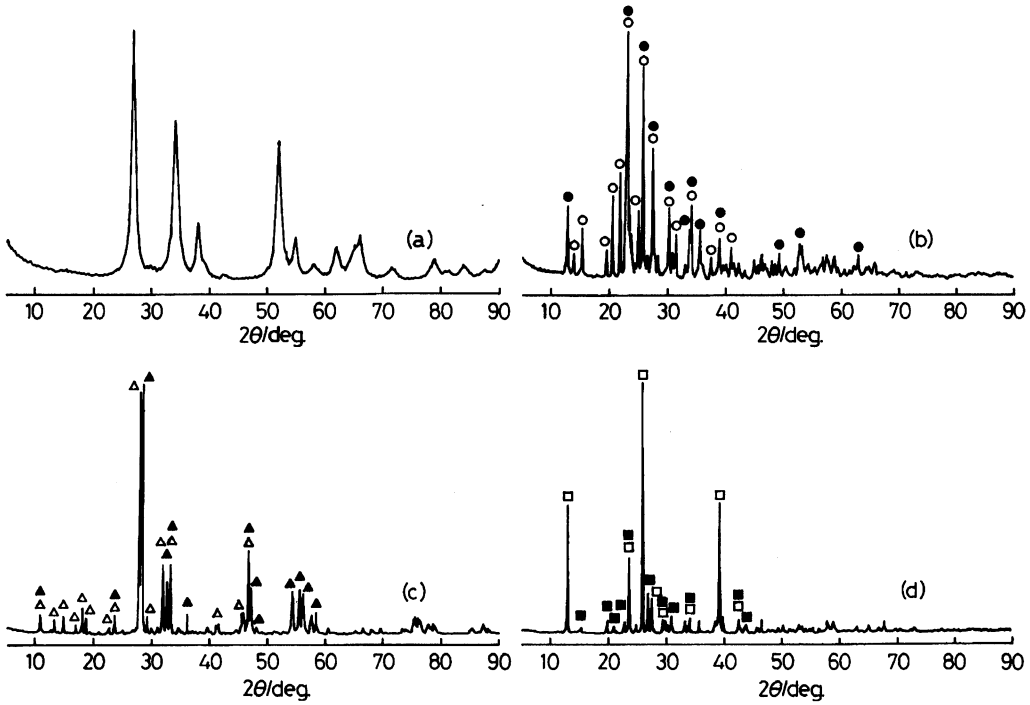

Fig. 4. Power X-ray diffraction patterns for binary oxide catalysts. (a) SnO_2–MoO_3, (b) Fe_2O_3–MoO_3, (c) Bi_2O_3–MoO_3, and (d) TeO_2–MoO_3. ○, $Fe_2(MoO_4)_3$; ●, MoO_3; △, β-phase; ▲, γ-phase; □, MoO_3; ■, $MoTe_2O_7$.

MoO_3. The selectivity to isopropyl pyruvate was much lower than that to **1b** as shown in Fig. 3. It is generally known that the oxidation behavior of higher alcohols is quite different from that of lower alcohols,[15] but we did not carry out further examination of the oxidation of isopropyl lactate on the catalyst.

Figure 4 shows powder X-ray diffraction (XRD) patterns for SnO_2–MoO_3, Fe_2O_3–MoO_3, Bi_2O_3–MoO_3, and TeO_3–MoO_3. All peaks detected for SnO_2–MoO_3 were assigned to tetragonal SnO_2 and nothing was indicated for the other component, MoO_3, which was confirmed by XPS as shown below. The XRD patterns for Fe_2O_3–MoO_3 revealed that the catalyst consisted of a mixture of MoO_3 and $Fe_2(MoO_4)_3$. Bi_2O_3–MoO_3 was $Bi_2O_3 \cdot 2MoO_3$ (β-phase) with $Bi_2O_3 \cdot MoO_3$ (γ-phase).[11] TeO_2–MoO_3 was s mixture of MoO_3 and $MoTe_2O_7$ and no TeO_2 was detected.

SnO_2–MoO_3. SnO_2–MoO_3 showed excellent reproducibility and the maximum yield at a low temperature of 250 °C. Furthermore, only SnO_2–MoO_3 among the various binary oxides examined showed activity in both the liquid-phase[8] and vapor-phase oxidation of **3b**. Therefore, the remainder of this report focuses on the results obtained with SnO_2–MoO_3. The reaction performance on SnO_2–MoO_3 was quite different from those on Fe_2O_3–MoO_3 and TeO_2–MoO_3 as shown in Fig. 5. The selectivity to **1b** on SnO_2–MoO_3 increased during the initial several hours to be an almost constant selectivity with a slight decrease in the conversion of **3b**. In contrast, the selectivity on Fe_2O_3–MoO_3 or TeO_2–MoO_3 showed high selectivity over 90% during 5 h on-stream. The acidity of SnO_2–MoO_3 is relatively high compared with the other catalysts examined (Table 1). Therefore, the acid sites on SnO_2–MoO_3 may decrease during the initial hours on-stream to show a similar acidity as that on Fe_2O_3–MoO_3 or TeO_2–MoO_3.

Increasing the partial pressure of O_2 from 5 to 10 mol% on SnO_2–MoO_3 showed a relatively little effect on both the conversion of **3b** and the selectivity to **1b**. It should be noted that the reaction of **3b** was observed in the absence of O_2 in the reactant gas to produce similar selectivities to **1a** and ethyl propionate with little formation of acetaldehyde as shown in Fig. 6. This means that reactions such as the dehydrogenation of **3b** to **1b**, hydrogenation of **3b** to ethyl propionate, and hydration of **1b** followed by decarboxylation to acetaldehyde occurred competitively. It was reported that the present SnO_2–MoO_3 with a Sn/Mo ratio of 9 possessed activities both for dehydrogenation and hydrogenation of 2-butanol in the presence of oxygen to afford 2-butanone and butenes, respectively.[15] Therefore, formation of a little acetaldehyde through the dehydration and the same selectivities to **1b** and ethyl propionate would suggest that most of the hydrogen from the dehydrogenation of **3b** to **1b** is consumed in the hydrogenation of **3b** to ethyl propionate competitively producing water. The present results may suggest that a lattice oxygen in the catalyst participates significantly in the reaction together with gas-phase oxygen. When the catalyst was calcined at 500 °C for 5 h in air, X-ray photoelectron spectra (XPS) gave the Mo $3d_{5/2}$ binding energy at 232.9 eV, characteristic of Mo(VI), with-

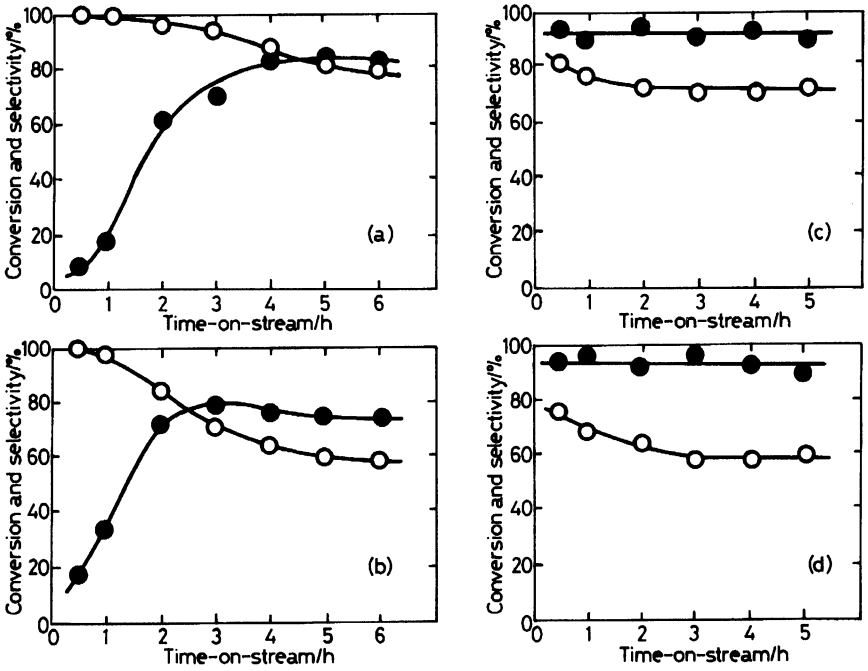

Fig. 5. Vapor-phase oxidation to ethyl lactate. (a) SnO_2–MoO_3, space time (θ)=3.6 s, 250 °C; (b) SnO_2–MoO_3, θ=2 s, 250 °C; (c) Fe_2O_3–MoO_3, θ=2 s, 280 °C; (d) TeO_2–MoO_3, θ=2 s, 300 °C. ○, Conversion of ethyl lactate; ●, selectivity to ethyl pyruvate.

out any appreciable chemical shift from the component MoO_3 observed at 233.2 eV as shown in Fig. 7 in good agreement with the literature.[15,16] It is of interest that the binding energy of Mo $3d_{5/2}$ shifted to 231.8 eV, after the catalyst was used for the reaction of **3b** in the absence of oxygen in the reactant stream. The binding energy was identified as Mo(V).[15] Further reduction of Mo(V) to Mo(IV) was not observed, since Mo(V) in the present SnO_2–MoO_3 was reported to be stable against reduction by H_2 treatment at 400 °C.[15] The present shift of Mo(VI) to Mo(V) would suggest that the lattice oxygen is supplied for the reaction as an oxygen source to reduce Mo(VI) to Mo(V). However, an appreciable shift for Sn $3d_{5/2}$ was not detected in the catalysts probably due to almost the same chemical shifts of Sn(IV) and Sn(II).[17]

In conclusion, the oxidation of ethyl lactate to pyruvate occurred selectively on MoO_3 and molybdenum-containing binary oxide catalysts. SnO_2–MoO_3 showed its maximum yield at a reaction temperature as low

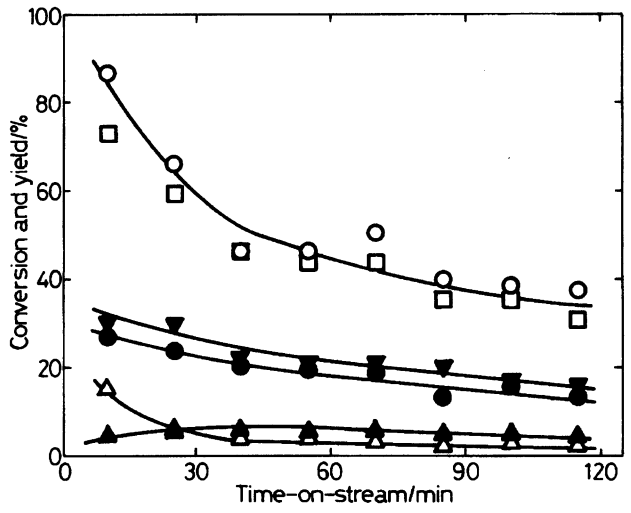

Fig. 6. Vapor-phase reaction of ethyl lactate in the absence of O_2 at 250 °C over SnO_2–MoO_3. ○, Ethyl lactate; ●, ethyl pyruvate; ▲, ethanol; △, acetaldehyde; ▼, ethyl propionate; □, acetaldehyde + ethyl pyruvate + ethyl propionate.

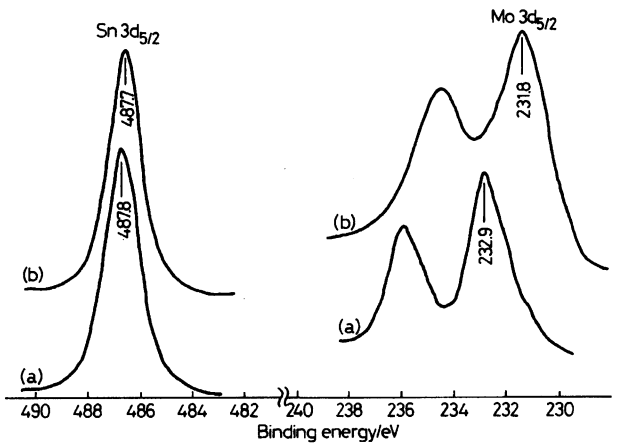

Fig. 7. X-Ray photoelectron spectra for SnO_2–MoO_3. (a) After calcination at 500 °C for 5 h in air. (b) After reaction in Fig. 6.

as 250 °C. XPS analysis for SnO_2–MoO_3showed that the lattice oxygen appears to participate in the reaction significantly together with gas-phase oxygen.

References

1) A. J. L. Cooper, J. Z. Gions, and A. Meister, *Chem. Rev.*, **83**, 321 (1983).
2) E. Erlenmeyer, *Ber.*, **14**, 320 (1881).
3) J. W. Howard and W. A. Fraser, "Organic Synthesis," 2nd ed, ed by H. Gilman, Wiley, New York (1948), Coll. Vol. 1, p. 475.
4) "The Merck Index-An Encyclopedia of Chemical and Drugs," 8th ed, ed by P. G. Stecher, Merck, Rahway, NJ (1968).
5) S. Sugiyama, S. Fukunaga, K. Ito, S. Ohigashi, and H. Hayashi, *J. Catal.*, **129**, 12 (1991).
6) S. Sugiyama, S. Fukunaga, K. Kawashiro, and H. Hayashi, *Bull. Chem. Soc. Jpn.*, **65**, 2083 (1992).
7) T. Tsujino, S. Ohigashi, S. Sugiyama, K. Kawashiro, and H. Hayashi, *J. Mol. Catal.*, **71**, 25 (1992).
8) H. Hayashi, S. Sugiyama, Y. Katayama, K. Sakai, M. Sugino, and N. Shigemoto, *J. Mol. Catal.*, in press (1993).
9) S. Tan, Y. Moro-oka, and A. Ozaki, *J. Catal.*, **17**, 132 (1970).
10) Y. Moro-oka, "Shokubai Chousei," ed by T. Shirasaki and N. Todo, Kodansha Scientific Pub., Tokyo (1974), p. 169.
11) I. Matsuura, "Shokubai Chousei Kagaku," ed by A. Ozaki, Kodansha Scientific Pub., Tokyo (1980), pp. 249—250.
12) Y. Takita, A. Ozaki, and Y. Moro-oka, *J. Catal.*, **27**, 185 (1972).
13) I. Matsuzaki, Y. Fukuda, T. Kobayashi, K. Kubo, and K. Tanabe, *Shokubai*, **11**, 210 (1969).
14) Y. Moro-oka, "Shokubai Chousei," ed by T. Shirasaki and N. Todo, Kodansha Scientigic Pub., Tokyo (1974), pp. 119—183.
15) Y. Okamoto, K. Oh-hiraki, T. Imanaka, and S. Teranishi, *J. Catal.*, **71**, 99 (1981).
16) T. A. Patterson, J. C. Carver, D. E. Leyden, and D. M. Hercules, *J. Phys. Chem.*, **80**, 1700 (1976).
17) C. D. Wagner, "Practical Surface Analysis by Auger and X-Ray Photolelctron Spectroscopy," ed by D. Briggs and M. P. Seah, John Wiley & Sons Ltd., Sussex (1983), Appendix 4.